Microvascular Research 80 (2010) 484–490

Contents lists available at ScienceDirect

Microvascular Research

journal homepage: www.elsevier.com/locate/ymvre

Regular Article

Tissue ACE inhibition improves microcirculation in remote myocardium after coronary stenosis: MR imaging study in rats

Karl-Heinz Hiller [b], Philipp Ruile [a], Günter Kraus [a], Wolfgang R. Bauer [a], Christiane Waller [c,*]

[a] Medizinische Klinik und Poliklinik I/Herz-Kreislauf-Zentrum, Würzburg, Germany
[b] MRB Research Center Magnetic-Resonance-Bavaria, Würzburg, Germany
[c] Psychocardiology, Medizinische Hochschule Hannover, Germany

ARTICLE INFO

Article history:
Received 18 January 2010
Revised 3 May 2010
Accepted 15 May 2010
Available online 4 June 2010

Keywords:
Microcirculation
ACE inhibition
Angiogenesis
Coronary stenosis

ABSTRACT

ACE inhibition has been shown to improve left ventricular (LV) and myocardial blood flow. Previous data regarding changes in capillary density and angiogenesis during ACE inhibition are controversial. The aim of the following study was to determine myocardial microcirculation and heart function in the rat after coronary stenosis using non invasive MR imaging techniques.

MR spin labeling and cine techniques have been performed in female Wistar rats 2 weeks after coronary artery stenosis. In one group, animals were treated with quinapril in a dose of 6 mg/kg/day. Perfusion, relative blood volume (RBV), LV mass and function were determined non-invasively 2 weeks after treatment. Finally, fibrosis and capillary density were analyzed histologically. Additionally, hemodynamic measurements were realized in a further group in order to calculate systemic vascular resistance (SVR).

Quinapril resulted in a significant increase in perfusion at rest in the remote and the poststenotic myocardium with improved systolic function and a decrease in SVR compared to the non treated control group. Additionally, maximum perfusion and RBV were slightly elevated whereas capillary density was unchanged among the groups.

MRI allows for non-invasive quantification of functional microcirculation and heart function. In addition to the well known effect of ACE inhibition on systolic function, treatment with the tissue specific ACE inhibitor quinapril revealed an important microvascular improvement, especially at arteriolar level. These findings may support the use of tissue ACE inhibitors to improve cardiac microcirculation after ischemia.

Introduction

Angiotensin-converting enzyme (ACE) inhibition is effective in reducing arterial blood pressure and left ventricular (LV) hypertrophy and in improving endothelial dysfunction and blood flow (Dietz et al., 1993; Lund-Johansen and Omvik, 1993; Tarazi and Zanchetti, 1985). However, previous data regarding changes in capillary density and angiogenesis during ACE inhibition are controversial. Captopril inhibited angiogenesis and microvascular growth in experimental tumors (Volpert et al., 1996) and in hypertensive and normotensive hearts (Wang and Prewitt, 1990) in the rat. However, spirapril has been shown to increase capillary density (Olivetti et al., 1993) and ramipril may augment capillary length density (Gohlke et al., 1996) in hypertensive rat hearts. Experiments in a rabbit model of hindlimb ischemia revealed that, in contrast to captopril treatment, tissue ACE inhibition by quinapril, which is known as one of the most efficient ACE inhibitors at tissue level, resulted in a stimulation of angiogenesis in vivo (Fabre et al., 1999). However, the functional significance of these microvascular changes relative to tissue mass is not well understood. Additionally, a study to investigate the influence of quinapril on microcirculation and angiogenesis in the heart muscle is lacking.

Besides morphometric analyses, there are only few methods for the quantitative analysis of microcirculation in the heart in vivo. Determination of perfusion is feasible using microspheres (Kowallik et al., 1991; Waller et al., 2005) or magnetic resonance imaging (MRI) (Jerosch-Herold et al., 2004; Belle et al., 1998). Relative blood volume (RBV) which reflects mainly the intracapillary blood volume in the heart is the second important parameter for the determination of functional microcirculation. RBV may be determined by echocardiography or MR techniques by use of an intravascular contrast agent (Jayaweera et al., 1999; Kahler et al., 1999). The magnetic resonance spin labeling technique enables to determine perfusion and RBV simultaneously (Waller et al., 2000). Principle of this technique is the detection of intrinsic changes in longitudinal relaxation (T_1) during the inflow of arterial blood in the myocardial tissue. In combination with the MRI measurement of left ventricular geometry and function,

* Corresponding author. Abteilung für Psychosomatik und Psychotherapie, Schwerpunkt Psychokardiologie, Medizinische Hochschule Hannover, Carl-Neuberg-Strasse 1, 30625 Germany. Fax: +49 511 532 3190.
E-mail address: waller.christiane@mh-hannover.de (C. Waller).

0026-2862/$ – see front matter © 2010 Elsevier Inc. All rights reserved.
doi:10.1016/j.mvr.2010.05.007

microcirculation may be determined relative to left ventricular mass and function.

The present study was carried out to investigate the effects of tissue ACE inhibition by quinapril on the microcirculation in the ischemic rat heart in vivo. Using MR imaging techniques adapted to small animal models, perfusion, intracapillary blood volume, left ventricular mass and function were determined during ACE-inhibition. In addition to these functional data, morphometric analyses of capillary density and myocyte hypertrophy were performed to investigate if quinapril may be able to stimulate angiogenesis in the ischemic heart.

Materials and method

Stenosis model and experimental preparation

The investigation conforms to the Guide for the Care and Use of Laboratory Animals published by the US National Institutes of Health (NIH Publication No.85-23, revised 1996) and was approved by the local authorities. Adult female Wistar rats (Charles River, Sulzfeld, FRG) weighing 260–310 g were used to induce coronary artery stenosis of the anterior descending branch of the left coronary artery (LAD). Therefore, a left thoracotomy was performed and the pericardium was incised. After exposure of the heart, a wire of 300 μm diameter was included into the ligation around the vessel 2–3 mm from its origin and quickly removed thereafter (Capasso et al., 1989). Sham operation was performed by the same surgical procedure without induction of coronary stenosis. Lethality of this procedure was 38% in the animals with coronary artery stenosis and 0% in the sham operated animals.

For MR and hemodynamic measurements anesthesia was induced by intraperitoneal injection of propofol (Disoprivan 2%, Glaxo Wellcome, Bad Oldesloe, Germany, 100 mg/kg i.p.) followed by oral intubation and artificial ventilation using a rodent respirator (BAS-7025, FMI, Germany). An electrically heating pad was used to maintain a constant body temperature of 37 ± 1 °C. Two tail veins were applied to maintain anesthesia by propofol (40 mg/(kg*min) and to induce vasodilation by adenosine (2 mg/(kg*min), Sigma-Aldrich, Taufkirchen, Germany). Phenylephrine (2.5–5 μg/(kg*min)) was additionally administered to maintain blood pressure and heart rate during vasodilation. A bolus injection of (Gd-DTPA)-albumin as an intravascular contrast agent (0.75 μmol/kg, ≈0.3 ml) was performed for RBV measurements (Ogan et al., 1987). MR images were acquired in end-diastole by triggering the ECG signal received via foreleg electrodes. Respiratory motion was eliminated by automatic arrest of respiration controlled by the pulse program (Kahler et al., 1998).

ACE inhibition was induced by oral administration of quinapril (Pfizer GmbH, Freiburg, Germany) in a dose of 6 mg/kg/day in 25 ml of drinking water followed by water ad libitum. Treatment started 6 h after operation and was stopped 1 day before the MRI experiment.

Experimental protocol

MR imaging was performed in 16 animals 2 weeks after sham operation (group 1) and in 16 animals 2 weeks after induction of coronary artery stenosis (group 2). Eight animals of each group were treated with the ACE inhibitor quinapril. Serum probes were collected prior to the MR experiments via a tail vein. MR measurements of perfusion and intracapillary blood volume were determined at rest and during vasodilation and left ventricular geometry and function (CINE MRI) were performed at rest. Finally, upon completion of in vivo MRI hearts were excised and MR coronary angiography was performed in isolated perfused hearts of group 1 according to Langendorff (1895), to confirm coronary stenosis as described by Nahrendorf et al. (2003). Therefore hearts were rapidly excised and perfused with nonrecirculating 37 °C Krebs–Henseleit buffer (concentrations in mmol/l: NaCl 118, KCl 4.7, $CaCl_2$ 1.75, $MgSO_4$ 1.2, KH_2PO_4 1.2, EDTA 0.5, $NaHCO_3$ 25, glucose 11) equilibrated with 95% O_2 and 5% CO_2 (pH = 7.4) at constant perfusion pressure (100 mmHg). A water-filled latex balloon was inserted in the left ventricle and connected to a Statham P23XL pressure transducer (Gould Inc., Oxnard, USA). The volume of the balloon was adjusted to an end-diastolic pressure of 5 mmHg. Left ventricular pressure was recorded by a PC to trigger MR-pulse sequences. Tissue samples of the isolated hearts were also used for histological staining.

Additional groups of 18 animals with sham operation (group 3) and of 18 animals with coronary stenosis (group 4) underwent MR CINE imaging at first. Ten animals of each group were treated with quinapril and eight animals were non-treated controls. Afterwards hemodynamic measurements were performed.

MR image acquisition

MRI acquisition was performed on a 7.05 T Biospec 70/21 spectrometer (Bruker, Ettlingen, Germany). A specially adapted whole body coil for transmission and a circular polarized surface coil as receiver were used to optimize signal acquisition in the rat heart in vivo (Kahler et al., 1998).

To assess the impact of coronary artery narrowing on myocardial perfusion and regional blood volume, quantitative T_1 imaging using an inversion recovery snapshot FLASH sequence was performed (Haase, 1990). 24 ECG-triggered snapshot FLASH images were recorded after global or slice selective spin inversion. Each snapshot FLASH image (TR = 2.25 ms, TE = 1 ms, flip angle about 3°, slice thickness 3 mm, field of view 50 × 50 mm) was acquired within a heart cycle (200–220 ms) with a consecutive spatial resolution of $390 \times 780\ \mu m^2$. Two successive ECG triggered T_1 experiments with different delays (varying in steps of 50–100 ms) between the inversion pulse and the first FLASH image were recorded in order to improve the time resolution of the T_1 measurement. This resulted in a total acquisition time for one T_1 image of 1–2 min ($2 \times 24 = 48$ FLASH images). Image acquisition was performed in the short axis view which was identified by axial and long-axis scout views.

For cine imaging, an ECG triggered fast gradient echo sequence was performed. Depending on heart rate, each cine image (flip angle 30°–40°, TE = 1.1 ms, TR = 3.2 ms, field of view 40 × 40 mm and 12 frames per heart cycle) had a total acquisition time of 40 to 50 s. The acquisition matrix was 128 × 128 resulting in a spatial resolution in plane of $310 \times 310\ \mu m^2$. Averaging the images four times resulted in an increase of the signal-to-noise ratio (SNR). Geometry and function were quantitatively determined by the acquisition of 16–20 contiguous ventricular short-axis slices of 1-mm thickness to cover the entire heart.

Three dimensional time of flight MR angiography was performed as described by Köhler et al. (2003) in an 11.7 T AMX-500 widebore magnet (Bruker, Karlsruhe, Germany). Coronary vessels were imaged by a mid-diastolic triggered segmented flow-compensated three-dimensional FLASH pulse sequence (flip angle 30°; TE = 1.3 ms; TR = 3.0 ms; acquisition matrix 128^3 data points; isotropic resolution of 140 μm) with eight phase encoding steps during one heart beat.

MR imaging of myocardial perfusion and intracapillary blood volume

Perfusion quantification was performed using a slice selective (sel) and a global (glob) T_1 experiment according to Eq. (1) where λ is the blood–tissue partition coefficient of water which is assumed to be 0.95 ml/g for blood perfused myocardial tissue (Belle et al., 1998).

The values for $T_{1,blood}$ were obtained from the pixels in the lumen of the left ventricular heart chamber of $T_{1,glob}$ maps.

$$\frac{P}{\lambda} = \frac{T_{1,glob}}{T_{1,blood}} \cdot \left(\frac{1}{T_{1,sel}} - \frac{1}{T_{1,glob}} \right). \quad (1)$$

From two slice selective T_1 experiments by the measurement of $1/T_{1,sel}$ before and after application of an intravascular contrast agent (ca) the intracapillary or regional blood volume (RBV) may be calculated following Eq. (2) (Kahler et al., 1999)

$$\frac{RBV}{\lambda} = \frac{\frac{1}{T_{1,sel}^{ca}} - \frac{1}{T_{1,sel}}}{\frac{1}{T_{1,blood}^{ca}} - \frac{1}{T_{1,blood}}}. \quad (2)$$

The theoretical model is described in detail elsewhere (Bauer et al., 1996, 1997).

MR image analysis

Perfusion and intracapillary blood volume

T_1 maps were used to determine differences of perfusion or RBV between a control region and hypoperfused regions in the LV free wall within the same heart. Mean values for perfusion and RBV were obtained by averaging the pixel data in the manually delineated regions of interest (ROI). In sham operated animals, a mid-myocardial region of interest (ROI) covering the whole left ventricle was delineated (170–200 pixels). In the animals with coronary artery stenosis, the first ROI covered the remote left ventricular myocardium (120–160 pixels). The second ROI covered the poststenotic myocardium (30–50 pixels).

Global left ventricular function and mass

Myocardial and ventricular slice volumes were determined from end-diastolic (largest LV diameter) and end-systolic (smallest LV diameter) images by multiplication of the compartment area and slice thickness (1 mm) by use of an operator-interactive threshold technique. Absolute LV cavity volumes were calculated in end-diastole (EDV) and end-systole (ESV) as the sum of all blood pool areas. For LV mass measurement, epicardial and endocardial borders of all slices were delineated and the mass was defined as the volume within the borders multiplied by a factor of 1.05 which represents the myocardial specific density (g/cm^3). Stroke volume (SV) and ejection fraction (EF) were calculated (SV = EDV − ESV and EF = SV/EDV). Cardiac output (CO) was determined from SV*HR.

Three-dimensional angiography

For visualization of the vessel structure maximum intensity projection and surface rendering was used (AMIRA Graphics Software Package, Visar Imaging, San Diego, USA) after zero-filling the raw data.

Hemodynamic studies

Hemodynamic studies were performed 2 weeks after sham operation or coronary artery stenosis. Therefore, rats were prepared as described above. Mean aortic pressure (MAP) and heart rate (beats/min) were measured by use of a polyethylen catheter (Portex, Kent, Great Britain) connected to a Millar micromanometer (Millar Instruments, Houston, USA). Data were recorded at rest and during infusion of adenosine following the experimental setup of the animals measured by MR. Systemic vascular resistance (SVR) was calculated from MAP and MR data of cardiac output according to SVR = MAP/CO.

Measurement of serum levels of ACE activity

Serum ACE levels were determined by spectrophotometry using a Sigma diagnostic kit (Sigma-Aldrich). Hydrolysis of synthetic tripeptide substrate *N*-[3-(2-furyl)acryloyl]-L-phenylalanylglycylglycine (FAPGG) by ACE results in a decrease in absorbance at 340 nm. One unit of ACE activity is defined as the amount of enzyme that will catalyze formation of 1 μmol of furylacryloylphenylalanine (FAP)/min under the conditions of assay. ACE activity of the samples is determined relative to the sample reaction rate of the ACE calibrator.

Histology and immunohistochemistry

Tissue samples and histological staining

Hearts were excised and perfused with physiological saline solution and fixed in 6% formaldehyde for 24 h, sectioned perpendicular to its longitudinal axis, then dehydrated and embedded in paraformaldehyde. Sections 1–2 μm in thickness were obtained with a microtome blade (10 cm long, PFM, Köln, Germany) using a rotary microtome (Microm HM400R, Walldorf, Germany). Tissue from the poststenotic myocardium that covered approximately 3 mm similar to the MR imaging slice were stained with hematoxylin and eosine for the morphometric analysis of reparative fibrosis and of myocyte cross sectional areas.

Immunohistochemical staining of endothelial cells

Poststenotic myocardial sections corresponding to the MR imaging slice were incubated with biotin-conjugated lectin (Bandeiraea simplicifolia BS-I, Sigma, 1:200 dilution in PBS) for 60 minutes at room temperature. Streptavidin-peroxidase complex and diaminobenzidin (DAB) as a substrate (Zymed, San Francisco, CA) were used to visualize binding of lectin.

Quantitation of fibrosis, myocyte cross sectional areas and capillary densities

Image analysis was performed in the remote myocardial tissue by microscopy (Carl Zeiss, Göttingen, Germany) using an analytical system (Visitron Systems, Puchheim, Germany). Three sections stained for hematoxyline and eosine were analyzed at a magnification of ×2.5. The volume fractions of fibrotic lesions were calculated as the average of the three sections and expressed as a percentage of the whole left myocardium. From these sections, myocyte cross sectional areas were determined in 20 independent field of views for each section at a magnification of ×32. Therefore, only cross sectioned myocytes with a central nucleus and 4–5 surrounding capillaries were used and the cross sectional area of each myocyte was manually delineated. Twenty independent field of views for each section were analyzed for capillary densities at a magnification of ×32. Endothelial cells were sectioned perpendicular to their longitudinal axes, manually counted and expressed as capillary endothelial cells/mm^2.

Statistical analysis

The data are expressed as mean ± SEM. Statistical tests were evaluated by ANOVA (InStat, GraphPad, San Diego, USA). Data were regarded as different when two-tailed P values in t-tests were less than 0.05.

Results

Serum ACE activity

ACE activity of the quinapril treated animals was suppressed to 35.8 ± 6.5 U/l in the serum of the animals used for MRI and to 40.4 ± 7.1 U/l in those used for hemodynamic studies. Non-treated animals had serum ACE activities of 107.3 ± 7.9l and 110.0 ± 6.1 U/l in the animals used for MRI and in the animals for hemodynamic studies, respectively ($p<0.001$ compared to the quinapril treated animals).

Magnetic resonance imaging

Quantitative results of perfusion (in ml/g/min) and RBV (in %) in the animals with coronary artery stenosis and sham operation of the quinapril treated and non-treated groups are shown in Fig. 1A/B.

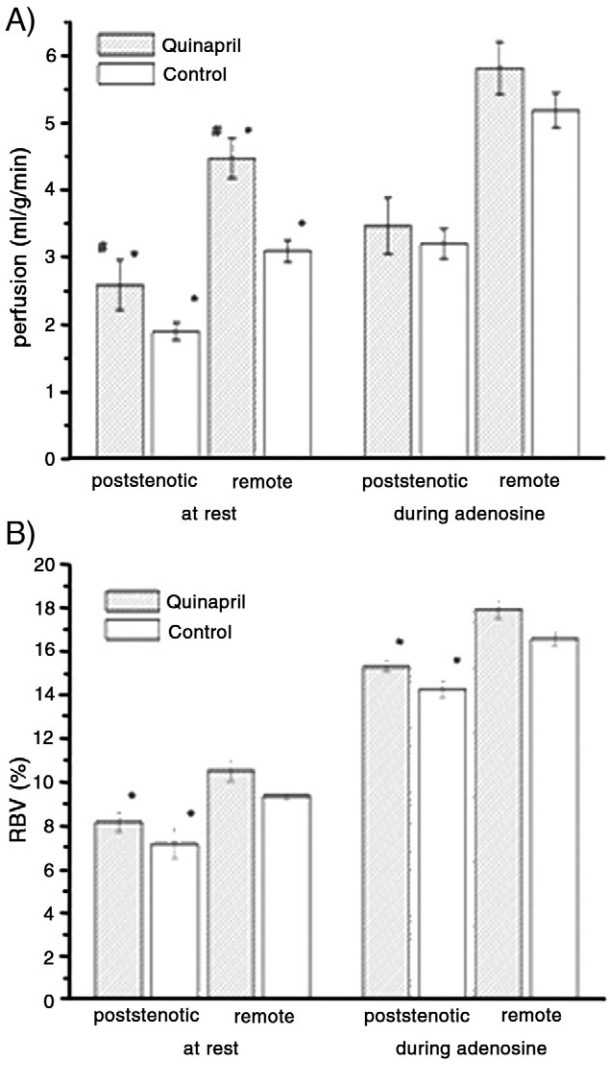

Fig. 1. Quantitative data (mean ± SEM) of myocardial perfusion and intracapillary blood volume obtained by MR imaging of the animals with 2 weeks coronary stenosis. Data are shown separately for the poststenotic area and the remote myocardium at rest and during vasodilatation. Perfusion is expressed in ml/g/min. RBV is expressed in Vol% (#$p<0.01$, quinapril vs. control, *$p<0.01$, at rest vs. during vasodilatation).

Perfusion at rest of the animals with quinapril treatment was significantly increased compared to the non-treated animals ($p<0.05$). However, maximum perfusion and values for intracapillary blood volumes showed no significant difference between the quinapril and the non-treated groups. In the sham operated animals, perfusion (4.16 ± 0.12) and RBV (10.12 ± 0.22) in the quinapril treated group at rest were significantly elevated ($p<0.05$) compared to their sham operated controls (3.17 ± 0.08 and 8.78 ± 0.27, respectively) whereas maximum values were slightly but not significantly increased (perfusion: 6.02 ± 0.28 vs. 5.11 ± 0.27, RBV: 18.20 ± 0.26 vs. 16.48 ± 0.44). Representative MR maps of myocardial perfusion and RBV of animals with coronary artery stenosis either under quinapril or no treatment at rest are shown in Fig. 2. Reduced perfusion and RBV in the anterior, poststenotic myocardium in the animals with coronary artery stenosis and the increased basal perfusion due to quinapril in the whole left myocardium are clearly visible. Quantitative results of global left ventricular geometry and function for both groups are shown in Table 1a/b. Quinapril treated animals with coronary artery stenosis showed a significant increase in SV and a higher EF compared to the non-treated animals ($p<0.05$).

Using 3D MR angiography coronary stenosis was clearly identified in all isolated rat hearts of group 2 (Fig. 3). A small signal void

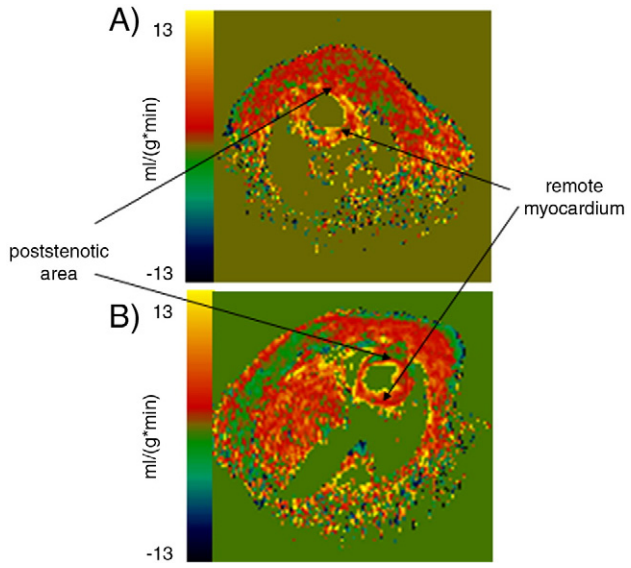

Fig. 2. Representative MR perfusion maps of two animals with coronary stenosis. A) Quinapril treated animal. B) Animal without treatment. The rat hearts are imaged in a short axis view. The remote myocardium in diastole is clearly visible (→). The right ventricular wall is rarely visible due to the thin myocardium (color scaling in $ml \cdot min^{-1} g^{-1}$). Poststenotic area is located adjacent to the anterior thorax of the animals (→). Myocardial perfusion is clearly elevated in the quinapril treated animal.

depending on the reduction of coronary cross section was caused by the higher flow in the ligated vessel region. Distal from the location of stenosis signal returns. In contrast infarcted hearts will show a complete signal loss at the site of ligation (Nahrendorf et al., 2003).

Morphometric data

Fibrotic areas in percent of the whole left ventricle in the poststenotic myocardial tissue of the animals with coronary artery

Table 1
Quantitative data of myocardial geometry and function of the sham animals (group 1) and animals with coronary stenosis (group 2) whether treated with quinapril or not.

a. MR cine data of sham operated animals

Group	Sham operated animals	
	Quinapril	Controls
Body weight (g)	265 ± 4	282 ± 5
LV mass/body weight (mg/g)	1.79 ± 0.04†	1.78 ± 0.06†
LV EDV (μl)	176.8 ± 10.3†	190.0 ± 14.1†
SV (μl)	124.0 ± 6.2	110.2 ± 7.4
EF (%)	71.4 ± 4.1	70.8 ± 3.4†
CO (ml/min)	37.6 ± 2.4	32.8 ± 3.8

LV, left ventricular. EDV, end-diastolic volume. SV, stroke volume. EF, ejection fraction, †$p<0.05$, vs. coronary artery stenosis.

b. MR cine data of animals with coronary artery stenosis

Group	Coronary artery stenosis	
	Quinapril	Controls
Fibrosis (%)	9.2 ± 1.9	5.7 ± 0.6
Body weight (g)	295 ± 4	274 ± 5
LV mass/body weight (mg/g)	1.93 ± 0.06	2.05 ± 0.08
LV EDV (μl)	273.9 ± 44.6	255.7 ± 38.6
SV (μl)	146.2 ± 6.3*	120.8 ± 11.8
EF (%)	60.3 ± 6.3#	50.2.1 ± 5.8
CO (ml/min)	47.0 ± 2.9	37.3 ± 3.0

LV, left ventricular. EDV, end-diastolic volume. SV, stroke volume. EF, ejection fraction.
*$p<0.01$ quinapril vs. controls, #$p<0.05$ quinapril vs. Controls, †<0.05 sham vs. coronary artery stenosis.

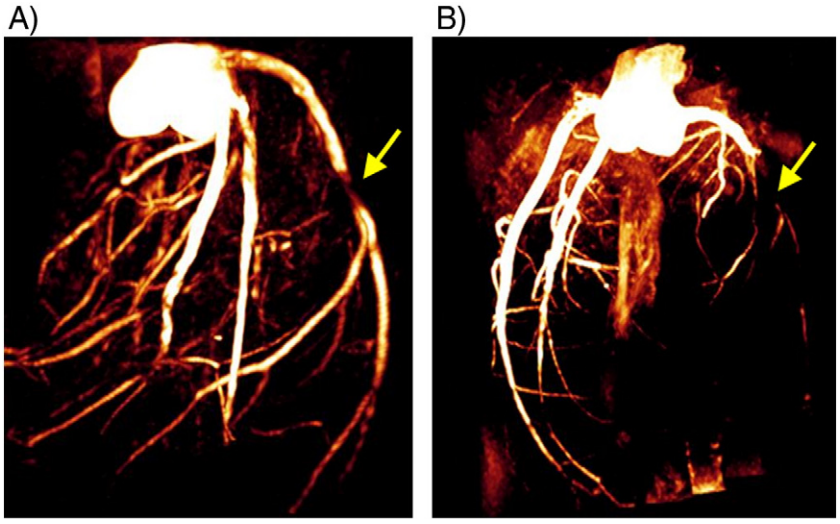

Fig. 3. Representative 3D MR angiography (MIP) was used to confirm status of coronary arteries in the isolated perfused rat heart. A) Angiography displays reduction of vessel cross section in the stenotic area (→) of a rat heart with 2 weeks coronary stenosis. B) In contrast angiography displays occlusion of the coronary artery, resulting in myocardial infarction.

stenosis were 9.17 ± 2.35% in the quinapril treated group and 7.51 ± 1.36% in the non-treated group. In the sham operated animals capillary densities were 4618 ± 185/mm^2 and 4571 ± 166/mm^2 in the treated animals and in the non-treated group, respectively. Capillary density in the animals with coronary artery stenosis was 4410 ± 116/mm^2 in the quinapril treated group and 4168 ± 121/mm^2 in the non-treated animals. In the non-treated animals, myocyte areas were 189 ± 6 and 194 ± 8 μm^2 in the animals with coronary stenosis and the sham operated group, respectively. Myocyte areas in the quinapril treated animals were 185 ± 6 μm^2 in the animals with coronary artery stenosis and 169 ± 5 μm^2 in the sham operated group.

Hemodynamic changes

In the quinapril treated animals, MAP and heart rate were slightly reduced at rest and showed a significant decrease during vasodilatation compared to the non-treated animals. Systemic vascular resistance was significantly reduced during vasodilation in the quinapril treated group compared to the control animals ($p<0.05$). The quantitative data of all groups are illustrated in Table 2.

Discussion

MR imaging of myocardial microcirculation allows to quantitatively visualize improved myocardial perfusion in both, remote and poststenotic rat myocardium, 2 weeks after coronary stenosis due to treatment with quinapril. Additionally, MR cine imaging revealed better quantitative systolic function in comparison to non-treated controls. The perfusion increase at rest rather reflects a decrease in systemic vascular resistance and improved systolic function. Quinapril as a tissue specific ACE-inhibitor has been shown to improve microcirculation and systolic function in a rat model of coronary artery stenosis.

Methodology

MR imaging has become the gold standard for the in vivo quantification of LV geometry and function in humans and small animal models (Higgins et al., 1988; Rerkpattanapipat et al., 2003). Additionally, several techniques have been evaluated for the quantitative measurement of myocardial blood flow and volume (Waller

Table 2
Hemodynamic data of sham operated animals (group 3) and animals with coronary stenosis (group 4) to compare hemodynamics between non-treated and quinapril treated animals.

	Sham operated animals		Coronary artery stenosis	
	Quinapril	Controls	Quinapril	Controls
BW (g)	285 ± 10	287 ± 8	308 ± 3	297 ± 4
Fibrosis (%)			9.2 ± 0.8	7.4 ± 0.6
LVSP (mmHg)	139 ± 7	149 ± 5	144 ± 9	134 ± 6
LVEDP (mmHg)	3.8 ± 0.5	2.7 ± 0.7	4.4 ± 0.8	6.3 ± 1.3*
LVDP (mmHg)	135 ± 7	146 ± 6	140 ± 9	128 ± 6
MAP (mmHg) at rest	119 ± 4†	127 ± 6†	112 ± 7†	120 ± 6†
MAP (mmHg) during vasodilation	68 ± 4#	85 ± 6	63 ± 4#	79 ± 5
HR (beats/min) at rest	331 ± 15†	387 ± 11†	319 ± 15#,†	364 ± 14†
HR (beats/min) during vasodilation	239 ± 10#	320 ± 21	221 ± 8#	290 ± 9
SVR (dyne*s)/cm^5 at rest	3285 ± 227†	2922 ± 265†	2479 ± 214#,†	3441 ± 307†
SVR (dyne*s)/cm^5 during vasodilation	2009 ± 231	1823 ± 215	1378 ± 105#	2300 ± 229
RPP (HR*(LVS P-LVEDP))	49606 ± 4359	57616 ± 2424	55670 ± 5273	46941 ± 3523

BW, body weight. LVSP, left ventricular systolic pressure. LVEDP, left ventricular enddiastolic pressure. LVDP, developed left ventricular pressure. MAP, mean aortic pressure. HR, heart rate. RPP, rate pressure product.
*$p<0.05$ coronary artery stenosis vs. sham operated animals. #$p<0.05$ quinapril vs. controls. †$p<0.01$ at rest vs. during adenosine.

et al., 2000; Sakuma and Higgins, 2004). In combination with hemodynamic data and MR data for CO, SVR may be determined from the same animal in order to evaluate vascular resistance. Using magnetic spin labeling techniques for perfusion and blood volume measurements in combinations with morphometry and vascular resistance in this study, the microcirculatory effects of tissue ACE inhibition may be determined non-invasively. Even though morphometric analysis of capillary density post mortem is unaltered, functional microcirculation may show important alterations due to arteriolar and capillary recruitment. Therefore, for the complete understanding of microvascular alterations and angiogenic processes, both, functional and morphological analyses have to be realized.

Effects of ACE inhibition

ACE inhibition has been widely shown to improve surviving rate and left ventricular function in a dose dependent manner (Pfeffer et al., 1985; Ertl et al., 1990) and to reduce apoptosis and fibrosis in different animal models (Kobara et al., 2003; Weber and Brilla, 1991). Additionally, ACE inhibition resulted in reduced LV hypertrophy (Clozel et al., 1989). In a chronic rat model of coronary stenosis, ACE inhibition resulted in an improvement of myocardial blood flow and reserve with consecutive better systolic and diastolic LV function (Sato et al., 2003). A better coronary reserve with reduced LV hypertrophy following long term ACE inhibition has also been shown in hypertensive animal models and patients (Clozel et al., 1989; Strauer et al., 1993; Buus et al., 2004). These effects have been related to a regression of hypertensive resistance artery structure and structural vascular abnormalities. These findings have been confirmed by our results. In our study, perfusion at rest and during maximum vasodilatation was improved in remote and poststenotic myocardium due to quinapril and systemic vascular resistances were reduced at rest and during maximum vasodilatation in the same animals.

Tissue ACE inhibition and angiogenesis

Additionally to the common effects of ACE inhibitors (Haleen et al., 1991), quinapril has been shown to be more effective in the ACE inhibition at the tissue level than other ACE inhibitors (Fabris et al., 1990). The administration of ACE inhibitors, especially those with high tissue affinity, resulted in proangiogenic effects by increasing microvessel density in animal models of experimental hypertension and hindlimb ischemia (Olivetti et al., 1993; Gohlke et al., 1996; Fabre et al., 1999). Only few studies focus on the differences in the ability to inhibit ACE in relevant tissues. ACE inhibitors can be divided into tissue specific or serum ACE inhibitors, however, there are only few studies which focus on the hypothesis that inhibition of tissue ACE may be important to obtain an optimal effect of ACE inhibitors. Some studies revealed a dose-dependent inhibition of vascular ACE activity versus plasma ACE-activity with inhibition of plasma ACE only with the highest dose (Buikema et al., 1997). In our study, tissue ACE inhibition using quinapril resulted in an improvement of microcirculation and systolic function which implies both, effects on tissue and plasma ACE activity.

ACE inhibition results in an augmented endothelial cell level of nitric oxide (NO). In a variety of studies, NO has been identified as an important regulatory molecule for angiogenesis [Waller et al., 2003, 2005]. In different in vivo models, chronic inhibition of nitric oxide synthesis resulted in microvascular remodeling and inhibition of angiogenesis (Matsunaga et al., 2000; Numaguchi et al., 1995; Ziche et al., 1994). In our study, morphometric analysis of capillary density revealed no significant changes in terms of proangiogenic effects due to quinapril. In contrast to our study design, treatment with ACE inhibitor in other studies was longer than 1 month. Therefore, structural treatment effects as capillary growth may be visible only at later time points.

Effects on poststenotic versus remote myocardium

Coronary artery stenosis in the rat heart leads to patchy necrosis in the poststenotic myocardium due to poor coronary collateralization (Capasso et al., 1989; Waller et al., 2003). Therefore, MR poststenotic myocardial perfusion is regularly composed of viable and scar tissue. Like in previous studies in large animals and humans (Fallavollita et al., 2003; Heusch, 1998), perfusion in viable poststenotic myocardium of rodent hearts is also reduced (Waller et al., 2005). In this study, quinapril has been shown to improve myocardial perfusion not only in the intact remote but also in the viable poststenotic myocardium. This effect was not related to a reduction of scar tissue due to ACE inhibition since fraction of replacement fibrosis was comparable in both groups.

Conclusions

Tissue ACE inhibition using quinapril results in an important functional improvement of myocardial microcirculation at rest in both, the remote and the poststenotic myocardial tissue of the rat heart post coronary stenosis. Additionally to the well known effects of ACE inhibition on cardiac function, this non invasive imaging study support findings of an improvement of myocardial microcirculation in the ischemic heart using tissue specific ACE inhibitors.

Funding

This work was supported in part by the Deutsche Forschungsgemeinschaft (Grant SFB688 and WA 1573/1-1) and by a grant from IZKF Würzburg (01 KS-9603).

Acknowledgments

We are grateful to Yvonne Vogt, Sabine Voll, Brigitte Schmitt and Charlotte Dienesch for their technical assistance in the experimental preparations.

References

Bauer, W.R., et al., 1996. Magnetization exchange in capillaries by microcirculation affects diffusion-controlled spin-relaxation: a model which describes the effect of perfusion on relaxation enhancement by intravascular contrast agents. Magn. Res. Med. 35, 43–55.

Bauer, W.R., et al., 1997. The effect of perfusion on T_1 after slice selective spin inversion in the isolated cardioplegic rat heart: measurement of a lower bound of intracapillary-extravascular water exchange rate. Magn. Res. Med. 38, 917–923.

Belle, V., et al., 1998. In vivo quantitative mapping of cardiac perfusion in rats using a noninvasive MR spin-labeling method. J. Magn. Reson. Imaging 8, 1240–1245.

Buikema, H., et al., 1997. Differential inhibition of plasma versus tissue ACE by utibapril: biochemical and functional evidence for inhibition of vascular ACE activity. J. Cardiovasc. Pharmacol. 29, 684–691.

Buus, N.H., et al., 2004. Myocardial perfusion during long-term angiotensin-converting enzyme inhibition or beta-blockade in patients with essential hypertension. Hypertension 44, 465–470.

Capasso, J.M., et al., 1989. Ventricular remodeling induced by acute nonocclusive constriction of coronary artery in rats. Am. J. Physiol. Heart Circ. Physiol. 257, H1983–H1993.

Clozel, J.P., et al., 1989. Effects of chronic ACE inhibition on cardiac hypertrophy and coronary vascular reserve in spontaneously hypertensive rats with developed hypertension. J. Hypertens. 7, 267–275.

Dietz, R., et al., 1993. Improvement of cardiac function by angiotensin converting enzyme inhibition. Sites of action. Circulation 87 (supp), IV108–IV116.

Ertl, G., et al., 1990. Influence of angiotensin-converting enzyme inhibition on cardiac function in myocardial infarction. Am. J. Cardiol. 65, 70G–73G.

Fabre, J.-E., et al., 1999. Tissue inhibition of angiotensin-converting enzyme activity stimulates angiogenesis in vivo. Circulation 99, 3043–3049.

Fabris, B., et al., 1990. Inhibition of tissue angiotensin-converting enzyme (ACE) in plasma and tissue. J. Cardiovasc. Pharmacol. 15, 6–13.

Fallavollita, J.A., et al., 2003. Hibernating myocardium retains metabolic and contractile reserve despite regional reductions in flow, function, and oxygen consumption at rest. Circ. Res. 92, 48–55.

Gohlke, P., et al., 1996. Vascular and cardiac protection by ramipril in spontaneously hypertensive rats: prevention versus regression study. Br. J. Clin. Pract. Suppl. 99, 1873–1879.

Haase, A., 1990. Snapshot FLASH MRI. Application to T_1, T_2 and chemical-shift imaging. Magn. Res. Med. 13, 77–89.
Haleen, S.J., et al., 1991. Effects of quinapril, a new angiotensin converting enzyme inhibitor, on left ventricular failure and survival in the cardiomyopathic hamster. Hemodynamic, morphological, and biochemical correlates. Circ. Res. 68, 1203–1312.
Heusch, G., 1998. Hibernating myocardium. Physiol. Rev. 78, 1055–1085.
Higgins, C.B., et al., 1988. Functional evaluation of the heart with magnetic resonance imaging. Magn. Reson. Med. 6, 121–139.
Jayaweera, A.R., et al., 1999. Role of capillaries in determining CBF reserve: new insights using myocardial contrast echocardiography. Am. J. Physiol. 277, H2363–H2372.
Jerosch-Herold, M., et al., 2004. Analysis of myocardial perfusion MRI. J. Magn. Res. Imaging 19, 758–770.
Kahler, E., et al., 1999. Perfusion-corrected mapping of cardiac regional blood volume in rats in vivo. Magn. Res. Med. 42, 500–506.
Kahler, E., et al., 1998. Quantitative regional blood volume studies in rat myocardium in vivo. Magn. Res. Med. 40, 517–525.
Kobara, M., et al., 2003. Effects of ACE inhibition on myocardial apoptosis in an ischemia–reperfusion rat heart model. J. Cardiovasc. Pharmacol. 41, 880–889.
Köhler, S., et al., 2003. Time-resolved flow measurement in the isolated rat heart: characterization of left coronary artery stenosis. Magn. Res. Med. 50, 449–452.
Kowallik, P., et al., 1991. Measurement of regional myocardial blood flow with multiple colored microspheres. Circulation 83, 974–982.
Langendorff, O., 1895. Untersuchung am überlebenden Säugetierherzen. Pflügers Arch. 61, 291–332.
Lund-Johansen, P., Omvik, P., 1993. Cardiac effects of ACE inhibition. J. Cardiovasc. Pharmacol. 22 (Suppl 1), 36–40.
Matsunaga, T., et al., 2000. Ischemia-induced coronary collateral growth is dependent on vascular endothelial growth factor and nitric oxide. Circulation 102, 3098–3103.
Nahrendorf, M., et al., 2003. Chronic coronary artery stenosis induces impaired function of remote myocardium: MRI and spectroscopy study in rat. Am. J. Physiol. Heart Circ. Physiol 285, H2712–H2721.
Numaguchi, K., et al., 1995. Chronic inhibition of nitric oxide synthesis causes coronary microvascular remodeling in rats. Hypertension 26, 957–962.
Ogan, M.D., et al., 1987. Albumin labeled with Gd-DTPA. An intravascular contrast-enhancing agent for magnetic resonance blood pool imaging: preparation and characterization. Invest. Radiol. 22, 665–671.
Olivetti, G., et al., 1993. Spirapril prevents left ventricular hypertrophy, decreases myocardial damage and promotes angiogenesis in spontaneously hypertensive rats. J. Cardiovasc. Pharmacol. 21, 362–370.
Pfeffer, M.A., et al., 1985. Survival after an experimental myocardial infarction: beneficial effects of long-term therapy with captopril. Circulation 72, 406–412.
Rerkpattanapipat, P., et al., 2003. Assessment of cardiac function with MR imaging. Mag. Res. Imaging Clin. N. Am. 11, 67–80.
Sakuma, H., Higgins, C.B., 2004. Magnetic resonance measurement of coronary blood flow. Acta Paediatr. Suppl. 93, 80–85.
Sato, H., et al., 2003. Attenuation of heart failure due to coronary stenosis by ACE inhibitor and angiotensin receptor blocker. Am. J. Physiol. 10, H359–H368.
Strauer, B.E., et al., 1993. ACE-inhibitors and coronary microcirculation. Basic Res. Cardiol. 88 (supp 1), 97–106.
Tarazi, R.C., Zanchetti, A., 1985. Prospectives for angiotensin converting enzyme inhibition in heart diseases. J. Hypertens. Suppl. 3, 99–103.
Volpert, O.V., et al., 1996. Captopril inhibits angiogenesis and slows the growth of experimental tumors in rats. J. Clin. Invest. 98, 671–679.
Waller, C., et al., 2005. Resting perfusion in viable myocardium distal to chronic coronary stenosis is reduced: characterization by magnetic resonance imaging and radiolabeled microspheres in the rat. Am. J. Physiol. 288, H 2588–H 2593.
Waller, C., et al., 2003. Microvascular adaptation to coronary stenosis in the rat heart in vivo: a serial magnetic resonance imaging study. Microvasc. Res. 48, 123–127.
Waller, C., et al., 2000. Myocardial perfusion and intracapillary blood volume in rats at rest and with coronary dilatation: MR imaging in vivo with use of a spin-labeling technique. Radiology 215, 189–197.
Wang, D.H., Prewitt, R.L., 1990. Captopril reduces aortic and microvascular growth in hypertensive and normotensive rats. Hypertension 15, 68–77.
Weber, K.T., Brilla, C.G., 1991. Pathological hypertrophy and cardiac interstitium. Fibrosis and renin–angiotensin–aldosterone system. Circulation 83, 1849–1865.
Ziche, M., et al., 1994. Nitric oxide mediates angiogenesis in vivo and endothelial cell growth and migration in vitro promoted by substance P. J. Clin. Invest. 94, 2036–2044.